CHARACTERIZATION OF SELF-MODULATION IN A PLASMA WAKEFIELD ACCELERATOR

J. Mezger*,[1], G. Demeter[2], L. Ranc[1], M. Bergamaschi[3], P. Muggli[1,3]
[1]Max Planck Institute for Physics, Munich, Germany
[2] Wigner Research Centre for Physics, Budapest, Hungary
[3]CERN, Geneva, Switzerland

Abstract

AWAKE uses a long relativistic proton bunch to drive wakefields in plasma. The amplitude of the wakefields increases along the plasma as the bunch undergoes self-modulation (SM). Wakefields are energy deposited in the plasma that must dissipate, a fraction of which is emitted as light. Light diagnostics measuring the amount of light emitted can be used to study the development of the wakefield amplitude along the plasma. A finite radius plasma column may influence wakefields, their energy balance and possibly the self-modulation process. To study these effects, the evolving plasma column radius has to be measured. Here we report on the use of light diagnostics in the absence of wakefields for this purpose.

INTRODUCTION

Charged particle bunches propagating through plasma drive wakefields by displacing plasma electrons [1]. Wakefields can be used for particle acceleration. The accelerating gradients sustained by wakefields can be several orders of magnitude higher than in RF-cavities. AWAKE uses a long relativistic proton bunch (400 GeV, 48 nC) as driver. To reach accelerating gradients on the order of 1 GeV/m, the proton bunch must undergo self-modulation [2]. For this purpose, a 10.3 m rubidium vapor plasma source is used [3]. The plasma is created by a laser pulse ($I_0 \sim 10\,\mathrm{TW/cm^2}$, $t_{pulse} = 120\,\mathrm{fs}$ (FWHM), $\lambda = 780\,\mathrm{nm}$, $\Delta\lambda \gtrsim 5\,\mathrm{nm}$ [4]) ionizing the rubidium atoms with an ionization fraction of 100 % [5]. This ensures density uniformity within 0.2 % [3] and enables control over the plasma density by means of controlling the vapor density. A characteristic of a laser ionized plasma is that the radius of the plasma column changes along the pulse propagation due to the evolution of the laser beam energy, radius and thus intensity. We show here that the time integrated light recorded by ten CMOS cameras placed along the 10.3 m plasma column is consistent with the amount of ionized Rb atoms calculated by a simple model for laser ionization through which the radius of the plasma column can be extrapolated. The setup for the experiment and details on the light diagnostic can be found in Ref. [6]. Measurements presented in this work are taken in the absence of wakefields.

LASER IONIZATION MODEL

We introduce the laser ionization model that is used to interpret the light measurements of the laser ionized plasma column. Figure 1 illustrates the influence of each component in the model. We use the same approach as in Ref. [6] with some modifications, mainly the inclusion of ionization in the sheath layer and self-focusing of the laser pulse. The model assumes a Gaussian transverse beam profile. The beam is described by the two sigma beam width $w(z) = w_0\sqrt{1 + M^4\left(\frac{z-z_0}{z_R}\right)^2}$, which is measured in vacuum at five locations within the Rayleigh length $z_R = \frac{\pi w_0^2}{\lambda}$. The beam quality factor is M = 1.33, the waist size is $w_0 = 1.6\,\mathrm{mm}$ and its location $z_0 = 5.42\,\mathrm{m}$ from the entrance of the Rb vapor column. Field ionization occurs above an intensity threshold I_{th} and produces a plasma of 100 % singly ionized Rb atoms. In vacuum, the radius where intensity $I(r) = I_0(z)e^{-\frac{2r^2}{w(z)^2}} \geq I_{th}$ is $r_0(z) = \sqrt{\frac{w(z)^2}{2}\ln\left(\frac{I_0(z)}{I_{th}}\right)}$ (red solid line Fig. 1). When propagating through rubidium vapor, $r_0(z)$ changes as the laser pulse looses energy to ionization and its intensity decreases.

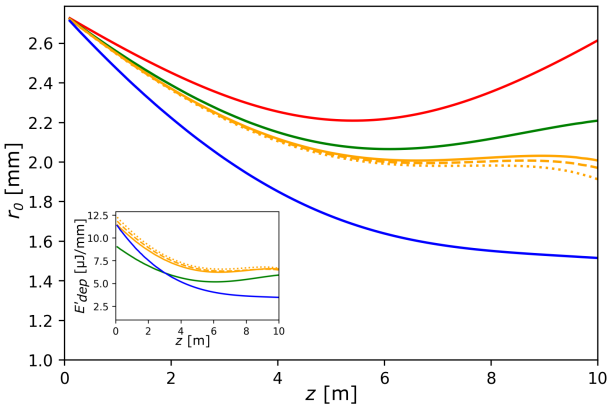

Figure 1: Plasma radius $r_0(z)$ (where $I(z,r) = I_{th}$) plotted against propagation distance of laser pulse z. Inset: Energy deposited in the vapor/plasma by the laser pulse per unit length. Red line: in vacuum. Green line: field ionization. Orange line: ionization in sheath layer. Orange dotted line: excitations in sheath layer. Orange dashed line: ponderomotive potential. Blue line: self-focusing.

First, we consider energy loss due to field ionization only. Over a distance Δz, the number of Rb atoms ionized through field ionization is $N_{ion,fi} = \pi r_0^2(z)\cdot\Delta z\cdot n_{rb}$, which requires energy $\Delta E_{fi}(z) = N_{ion,fi}\cdot e\phi_1$, where $e\phi_1 = 4.18\,\mathrm{eV}$ is the ionization potential and n_{rb} is the vapor density. We subtract the energy lost over a small step ($\Delta z = 1\,\mathrm{cm}$, $\Delta E_{fi} \ll E_{pulse}$) from the total energy of the pulse E_{pulse} and recalculate

* jan.mezger@cern.ch

$r_0(z)$ with smaller energy for the next step, thus propagating the pulse from the plasma entrance. We assume that the transverse beam profile remains Gaussian despite energy being absorbed only within $r < r_0$. This decreases the radius along the plasma (solid green line). The inset in Fig. 1 shows the corresponding energy deposited by the laser pulse per unit length $E'_{dep} = \frac{\Delta E_{fi}}{\Delta z}$.

Second, we consider that energy is also lost due to ionization in the so called sheath layer. For $r > r_0$, where $I < I_{th}$, three-photon ionization can occur with an ionization fraction $P < 100\,\%$. In the sheath layer the ionization fraction decreases exponentially as [7] $P_{3\gamma}(r) = P_{max} \exp(-\frac{(r-r_0)^2}{t_0^2})$ with a characteristic width t_0 ($P_{max} = 1$ when $I(r = 0) > I_{th}$). The width t_0 is related to the transverse intensity profile of the laser beam and therefore proportional to the evolving beam width $t_0(z) = t_0 \frac{w(z)}{w_0}$. Here, $N_{ion,sl} = (\sqrt{\pi} t_0(z) r_0(z) + t_0(z)^2)\pi \cdot \Delta z \cdot n_{rb}$ and the energy loss is $\Delta E_{sl} = N_{ion,sl} \cdot 3E_{ph}$, where $E_{ph} = 1.59\,\mathrm{eV}$ ($\lambda = 780\,\mathrm{nm}$). Adding this effect to the evolution of the laser beam envelope yields the orange solid line. Including ionization in the sheath layer significantly increases the energy deposited as shown in the inset, which in turn decreases the radius of the laser beam envelope, as the intensity of the laser pulse decreases.

The laser light ($\lambda = 780\,\mathrm{nm}$, $\Delta\lambda \gtrsim 5\,\mathrm{nm}$) is resonant with the D1, D2 (795, 780 nm from the ground state) and exited (776 nm) transitions of rubidium [7], so we also consider excitations to upper states that do not lead to ionization in the sheath layer. Because excitation probabilities, similar to ionization probabilities, usually scale to the power of the number of photons required [8], we assume that the excitation fractions to the first and second upper states scale as $P_{n\gamma} = P_{3\gamma}^{n/3}, n = 1, 2$. When compared to the orange solid line, the orange dotted line shows that this has a small effect and is not considered here after. Similarly, the effect of the ponderomotive potential was found negligible (orange dashed line), even when assuming that every ionized electron would gain the maximum energy from the potential.

Finally, we include non-linear focusing of the laser pulse. In the sheath layer, de-focusing due to plasma dispersion and focusing due to polarization of the rubidium atoms compete with each other, while the fully ionized plasma channel is practically transparent to the laser pulse. A full treatment of this effect is beyond the scope of this model. We therefore rely on empirical data to include this effect (data from Ref. [7]). We taper the beam width to match the measured width after propagation through vapor. The tapering is incorporated into the beam width as $w(z) = w_{vacuum}(z) \cdot (1 + \frac{z}{10\,\mathrm{m}}(\frac{w_{vapor}(10\,\mathrm{m})}{w_{vacuum}(10\,\mathrm{m})} - 1))$. A linear taper is chosen, as the real development of the pulse width due to self-focusing is unknown. Different tapering (quadratic/exponential) was tested and yielded worse results. Implementing this modification to the beam width yields the final beam envelope and energy deposition curve shown in blue, which we use for the rest of this work.

RESULTS

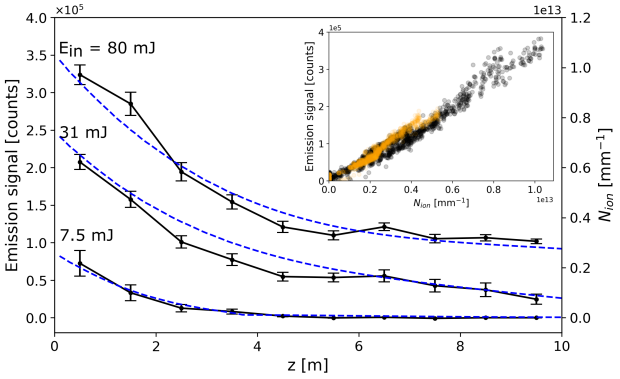

Figure 2: Measured emission signal (black symbols) and N_{ion} from the model (blue dashed lines) against propagation distance for different input pulse energies. Inset: Measured emission signal at any location against N_{ion} at corresponding location. E_{in} varied between 1 and 100 mJ with $n_{rb} = 1.95 \times 10^{14}\,\mathrm{cm}^{-3}$ (orange) and $3.85 \times 10^{14}\,\mathrm{cm}^{-3}$ (black).

For comparison of the model with light emission measurements, we use the number of ionized atoms over 1 mm (ROI of cameras is also 1 mm in z). The amount of light emitted depends only on the number of emitters (electron-ion pairs), which is approximately proportional to energy deposited by the laser pulse. This is because electrons are created with very little initial energy ($\overline{U}_{\mathrm{pondromotive}} \approx 0.2\,\mathrm{eV}$), so the only visible light emitted in the process is due to recombination. We adjust the free parameters of the model starting from theroetical / measured values ($I_{th} = 1.7\,\mathrm{TW/cm^2}$ [9], $t_0 = 0.2\,\mathrm{mm}$ [7], a = 1) and tuning them for best agreement with the data. We find: $I_{th} = 0.48\,\mathrm{TW/cm^2}$, which is lower than the theoretical value and can be explained by resonant excitation effects reducing the effective ionization threshold; $t_0 = 0.25\,\mathrm{mm}$ which is consistent values measured using schlieren imaging. For agreement with data, we need to multiply the energy loss at each step with a multiplication factor a. Here, $a = 1.5$ meaning that some energy loss is still not accounted for. However, this is an improvement compared to Ref. [6] where $a = 6.8$ showing that the modifications made yield a more physically consistent description. While previously, adjusting the parameters of the model could yield good agreement for measurements at one plasma density and one laser pulse energy, we can now find one set of parameters that fits measurements for several densities and pulse energies from 1 to 100 mJ.

Figure 2 shows measured light emission signals (black symbols) and N_{ion} calculated from the model (blue dashed lines) for input laser pulse energies $E_{in} = 80$, 31 and 7.5 mJ and $n_{rb} = 3.85 \times 10^{14}\,\mathrm{cm}^{-3}$. As expected, less pulse energy leads to less ionization and less light emitted / energy deposited. In all cases, the plasma column tapers down quickly for $z < 5\,\mathrm{m}$. For $E_{in} = 80\,\mathrm{mJ}$, the plasma column then remains essentially constant all the way to the plasma exit, as enough energy remains in the laser pulse to ionize the vapor. For $E_{in} = 31\,\mathrm{mJ}$, the plasma column tapers down to almost

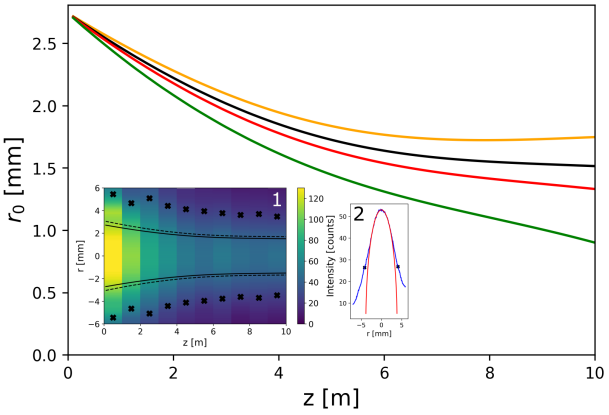

Figure 3: Radius of the 100 % ionized core of the plasma column against propagation distance for $n_{rb} = 1.95\times10^{14}$ cm^{-3} (orange), 3.85×10^{14} cm^{-3} (black), 4.9×10^{14} cm^{-3} (red) and 6.8×10^{14} cm^{-3} (green) with $E_{in} = 100$ mJ. Inset 1: Transverse profiles of the ten cameras stitched together. FWHM of transverse profiles (black symbols) and 100 % ionized core of the plasma column (black solid line) with sheath layer (black dashed line). Inset 2: Transverse profile at $z = 4.5$ m (blue) with a fit of the projection of a cylinder (red) and FWHM (black symbols).

zero radius at $z = 10$ m, as the laser pulse looses nearly all of its energy. For $E_{in} = 7.5$ mJ, the laser pulse loses all of its energy over $z = 0$ m to 5 m and does not ionize a plasma column after that. In all three cases, we observe relatively good agreement between the measurement and the model. We can quantify the agreement by plotting the measured emission signal at any of the ten locations against the model prediction for N_{ion} at that location (Inset Fig. 2) for all measurements with $E_{in} = 1$ mJ to 100 mJ and $n_{rb} = 3.85\times10^{14}$ cm^{-3} (black) and 1.95×10^{14} cm^{-3} (orange). The Pearson correlation coefficient between the measured emission signals and N_{ion} calculated from the model is 0.985 indicating a strong linear correlation. This suggests that the model is a good representation of the measurements.

We use the model to analyze the radius profiles of the 100 % ionized core of the plasma column. Figure 3 shows the profiles for $n_{rb} = 1.95\times10^{14}$ cm^{-3} (orange), 3.85×10^{14} cm^{-3} (black), 4.9×10^{14} cm^{-3} (red) and 6.8×10^{14} cm^{-3} (green) with $E_{in} = 100$ mJ. These are realistic parameters for self-modulation experiments at AWAKE. At the plasma entrance the radius is the same for all densities, about 2.7 mm. This is because the initial intensity profile of the laser pulse is the same and the threshold for field ionization does not depend on density. In all cases, the plasma radius tapers down over the first few meters, as the waist of the laser beam is close to the middle of the vapor column. For higher plasma densities, the tapering is steeper because the laser pulse looses more energy and self-focusing effects are stronger. This is more visible towards the plasma exit. Here, the plasma radius remains essentially constant for lower plasma densities, but keeps tapering down for higher ones.

We can compare the radii we obtain from the model with the transverse profiles from the camera images. Inset 1 shows the transverse profiles of the ten camera images stitched together. A larger plasma column appears both wider and brighter, because its height and depth increase. We observe less intensity and narrower profiles with increasing propagation distance. This is consistent with the model. However, the radius at half maximum (black symbols) is significantly larger than the model prediction (black solid line). Looking at a single profile (Inset 2, blue line), we also observe that it does not match the projection of a cylinder (red line) for large radii. This could be explained by the sheath layer smearing out the edges of the plasma. However, the plot of $r_0(z) + t_0(z)$ (black dotted line) does not explain the difference in transverse extent. More importantly, using schlieren imaging it was recently shown that the plasma expands transversely on the timescale of a few microseconds [10]. This means that emitters can move from their original location, effectively widening the observed plasma column. The exposure time of the cameras (40 µs) is much longer than the timescales of plasma expansion. Therefore, transverse profiles appear wider, while the total amount of light collected by the cameras is only affected by the relatively small number of emitters traveling far enough to leave the ROI.

For $n_{rb} = 4.9\times10^{14}$ cm^{-3} and 6.8×10^{14} cm^{-3}, we can compare the values of r_0 at the plasma exit with measurements from schlieren imaging presented in Ref. [7]. The model predicts radii $r_0(z = 10\,\text{m}, E_{in} = 100\,\text{mJ}) \approx 1.3$ mm and 0.9 mm respectively (Fig. 3), while the experimental values are approximately 1.3 mm and 1.1 mm. This shows that the values for r_0 extracted from the model are close to those measured before, while the values extracted from the camera images are larger than expected.

CONCLUSION

We presented a model for laser ionization of rubidium vapor which assumes a Gaussian beam profile, field ionization, three-photon ionization in the sheath layer and linear tapering of the beam width due to self-focusing effects. We optimized the parameters of the model by comparing the number of ionized Rb atoms with light emission measurements. The model was used to generate plasma radius profiles for several densities. The results can be used to include the effect of a tapering plasma channel on the wakefields driven by a self-modulating proton bunch in numerical simulations.

REFERENCES

[1] P. Chen, J. M. Dawson, R. W. Huff, and T. Katsouleas, "Acceleration of electrons by the interaction of a bunched electron beam with a plasma", *Physical Rev. Lett.*, vol. 54, no. 7, p. 693, 1985. doi:10.1103/PhysRevLett.54.693

[2] N. Kumar, A. Pukhov, and K. Lotov, "Self-modulation instability of a long proton bunch in plasmas", *Phys. Rev. Lett.*, vol. 104, no. 25, p. 255003, 2010. doi:10.1103/PhysRevLett.104.255003

[3] E. Öz and P. Muggli, "A novel Rb vapor plasma source for plasma wakefield accelerators", *Nucl. Instrum. Methods Phys. Res. A*, vol. 740, pp. 197–202, 2014. doi:10.1016/j.nima.2013.10.093

[4] V. Fedosseev *et al.*, "Integration of a terawatt laser at the CERN SPS beam for the AWAKE experiment on proton-driven plasma wake acceleration", CERN, Geneva, Switzerland, Rep. CERN-ACC-2016-209, 2016.

[5] AWAKE Collaboration *et al.*, "Experimental observation of proton bunch modulation in a plasma at varying plasma densities", *Physical Rev. Lett.*, vol. 122, no. 5, p. 054802, 2019. doi:10.1103/PhysRevLett.122.054802

[6] J. Mezger *et al.*, "Implementation of light diagnostics for wakefields at AWAKE", *Nucl. Instrum. Methods Phys. Res. A*, vol. 1075, p. 170426, 2025. doi:10.1016/j.nima.2025.170426

[7] G. Demeter *et al.*, "Generation of 10-m-lengthscale plasma columns by resonant and off-resonant laser pulses", *Opt. Laser Technol.*, vol. 168, p. 109921, 2024. doi:10.1016/j.optlastec.2023.109921

[8] R. W. Boyd, "Chapter 13 - ultrafast and intense-field nonlinear optics", in *Nonlinear Optics*. Cambridge, MA, USA: Academic Press, 2020, pp. 541–568. doi:10.1016/B978-0-12-811002-7.00022-9

[9] S. J. Augst, "Tunneling ionization of noble gas atoms using a high-intensity laser at 1 µm wavelength", Ph.D. thesis, University of Rochester, Rochester, NY, USA, 1991.

[10] J. Page, "Schlieren imaging at AWAKE", MA thesis, Technical University of Munich, München, Germany, 2026.